Synthesis and characterization of single-crystal indium nitride nanowires

Tao Tang, Song Han, Wu Jin, Xiaolei Liu, Chao Li, Daihua Zhang, and Chongwu Zhou[a)]
Department of E.E.-Electrophysics, University of Southern California, Los Angeles, California 90089

Bin Chen and Jie Han
Eloret Corporation, MS 229-1, NASA Ames Research Center, Moffett Field, California 94035

M. Meyyapan
NASA Ames Research Center, Moffett Field, California 94035

(Received 18 June 2003; accepted 21 November 2003)

InN nanowires were synthesized and characterized using a variety of techniques. A two-zone chemical vapor deposition technique was used to operate the vapor generation and the nanowire growth at differential temperatures, leading to high-quality single-crystalline nanowires and growth rates as high as 4–10 μm/h. Precise diameter control was achieved by using monodispersed gold clusters as the catalyst. Photoluminescence and Raman studies have been carried out for the InN nanowires at room temperature. Devices consisting of single nanowires have been fabricated to explore their electronic transport properties. The temperature dependence of the conductance revealed thermal emission as the dominating transport mechanism.

Nanostructured semiconducting III-V nitrides have long been viewed as promising materials for electronic and optoelectronic applications.[1] Among them, InN is particularly interesting because of its direct bandgap of 1.89 eV, which offers enormous promise for applications in photonic devices such as lasers, light emitting diodes in visible light range, and high-efficiency solar cells.[2] Furthermore, InN has distinct advantages over GaN for high-frequency field-effect transistor applications because of its superior transport characteristics.[3] InN nanostructures such as nanowires are therefore particularly tantalizing due to the potential of integrating the above-mentioned properties with various quantum effects. However, unlike the intensive effort spent on GaN nanowires,[4] the study of InN has not reached the same extent due to its low dissociation temperature, making the synthesis of high-quality InN nanowires very difficult. This is evident in the scarce report on InN nanowire synthesis. Zhang et al.[5] reported synthesis of InN nanowires using a vapor-solid approach without any catalyst; however, this approach yielded inhomogeneous nanowires with a broad diameter distribution of 10–100 nm. InN nanowires have also been synthesized via a vapor-liquid-solid (VLS) approach using a single-zone furnace at 500 °C,[6] and a diameter distribution from 40 to 80 nm was obtained. This lack of precise diameter control shared by those two synthesis techniques[5,6] poses a great threat to electronic and optoelectronic applications of InN nanowires. In addition, one drawback of the reported VLS approach[6] is the slow growth rate, as 8 h was used for producing micro-long nanowires. This severely hinders the synthesis of bulk-quality InN nanowires and is likely limited by the inefficiency in breaking NH_3 molecules at the relatively low synthesis temperatures used. Moreover, studies on the electronic properties of InN nanowires have not been reported thus far. Here we present use of a two-zone furnace for InN nanowire synthesis. This technique allowed us to use a high-temperature zone (700 °C) to break NH_3 molecules and a low-temperature zone to facilitate the nanowire growth. Our method produced single-crystalline nanowires with a high growth rate (4–10 μm/h) and precisely controlled diameters by using monodispersed gold clusters as the catalyst. In addition, photoluminescence and Raman studies have been carried out for the InN nanowires at room temperature. Furthermore, devices based on individual InN nanowires have been fabricated and their electronic transport properties were investigated for the first time.

The synthesis of InN nanowires is introduced as follows. The experimental setup for InN nanowire growth is depicted schematically in Fig. 1(a). A mixture of 8.4 mg of indium metal and 4.1 mg In_2O_3 (mole ratio 5:1), serving as the starting material, was placed in a quartz boat located inside a 1-inch-diameter quartz tube reactor. Si/SiO_2 substrates decorated with monodispersed 20-nm

[a)]Address all correspondence to this author.
e-mail: chongwuz@usc.edu

 © 2004 Materials Research Society

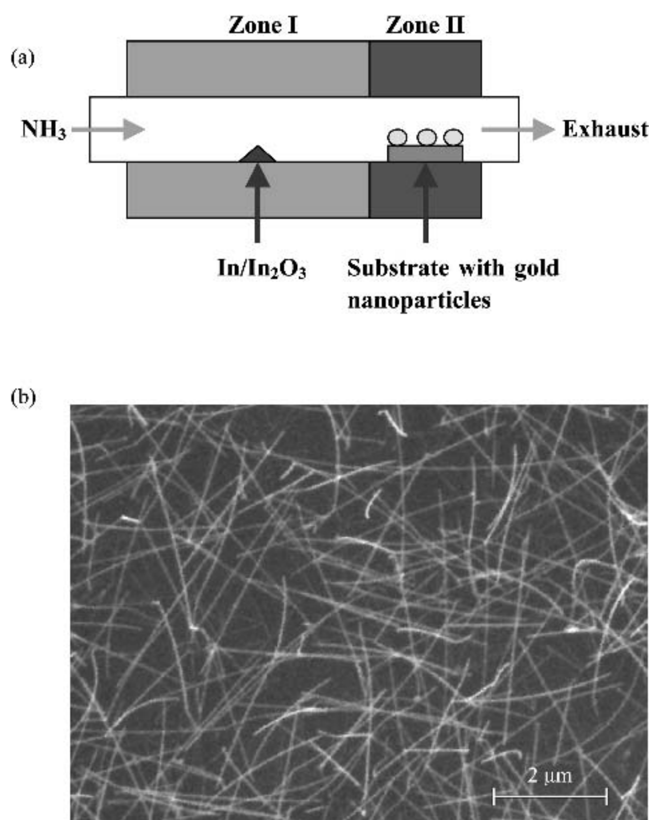

FIG. 1. (a) Schematic diagram of a two-zone CVD system for InN nanowire growth. (b) A typical SEM image of InN nanowires grown on a Si/SiO_2 substrate.

gold clusters were prepared as described previously.[7] These substrates were then placed at the downstream of the tube reactor separated from the starting material by 4 inches. Prior to heating up the reactor, the quartz tube was fully evacuated and then purged with high-purity argon for 10 min. The temperature of the In/In_2O_3 source zone (zone I) was set at 700 °C and the substrate zone (zone II) was set at 525 °C. Upon stabilization of the desired temperatures, the reaction was carried out by introducing anhydrous ammonia into the tube at a flow rate of 50 standard cubic centimeters per minute. The typical reaction time used was about half an hour. The Si/SiO_2 substrates were unloaded after cooling down, and later on characterized using scanning electron microscopy (SEM), transmission electron microscopy (TEM), and selected-area electron diffraction (SAED). Our synthesis is suggested to follow the VLS growth mechanism.[8] Vapor generated from the heated starting material first diffused into the gold catalytic clusters and formed Au/In alloy droplets. Continued supply of indium vapor then led to supersaturation of the Au/In droplets and subsequently nucleation of the indium phase. In the mean time, thermally decomposed NH_3 served as a source of nitrogen radicals, which can react with the In separated out of the Au/In alloy and lead to the growth of InN nanowires along the longitudinal direction. Consequently, the diameter of the InN nanowires should be directly linked to the catalytic particle size. The temperature of hot zone I was carefully chosen under the consideration of providing the right amounts of both indium vapor and nitrogen radicals whereas the temperature of hot zone II, where the substrates were located, was selected based on the thermal stability of InN and the formation of Au/In alloy. We can therefore achieve high-quality single-crystalline nanowires as well as high growth rates.

A typical SEM image of the InN nanowires grown from 20-nm gold clusters is shown in Fig. 1(b). These nanowires covered the whole substrate and appeared to be uniform in both diameter and length. Detailed TEM and SEM examination showed that these nanowires have diameters around 20 nm and lengths of 2–5 μm with aspect ratios exceeding 100:1. Our results infer a growth rate of 4–10 μm/h, indicating an ample supply of nitrogen radicals can be achieved with our two-zone setup. Figure 2 presents a TEM image of a single InN nanowire, where an Au/In alloy particle about 20 nm in diameter can clearly be seen at the very tip as a result of the VLS growth mechanism. The Au/In alloy nanoparticle appears darker than the InN nanowire due to the larger electron scattering cross-section of the Au atom than that of InN. The nanowire looks rather homogenous, suggesting single-crystalline structures for our nanowire. The upper-left inset in Fig. 2 shows a SAED pattern recorded perpendicular to the nanowire long axis. Similar diffraction patterns were consistently observed for many nanowires and also at different positions of the nanowires. These observations further confirmed the single-crystalline nature of our nanowires. The pattern can be indexed to the diffraction pattern of Wurtzite InN with a lattice constant $a = 3.67$ Å, $c = 5.79$ Å, in agreement with that of bulk InN ($a = 3.533$ Å, $c = 5.693$ Å).[9] Comparing the indexed pattern and the corresponding TEM image with field rotation correction, we found that our nanowires preferably grew along the [110] direction, which is in agreement with Ref. 6 and implies that growth along [110] has the lowest free energy. Further insight into the structure of the as-grown InN nanowire was provided by the high-resolution TEM image [Fig. 2(b)]. The clear lattice fringes indicate the single-crystalline nature of the nanowire. The distance of 0.579 nm between the adjacent lattice planes corresponds to the planar spacing between two (001) crystal planes. This suggests the growth direction is perpendicular to [001] direction, which is consistent with what we obtained from the diffraction pattern. In addition, to demonstrate our control over the nanowire diameters, the diameter distribution of as-grown InN nanowires was carefully investigated by TEM inspection of 30 nanowires, with the histogram plotted in the lower inset of Fig. 2. A Gaussian curve fitting based on this histogram (solid curve) yields a mean diameter of

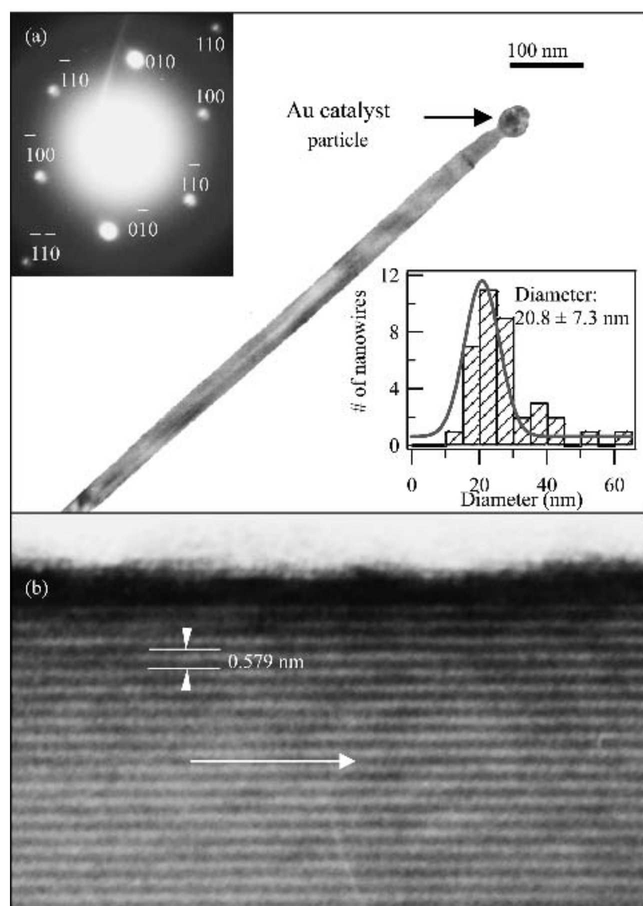

FIG. 2. (a) TEM image of an InN nanowire with a Au catalytic particle at the tip. The growth is along the [110] direction. Upper-left inset: electron diffraction pattern of the nanowire revealing the Wurtzite crystal structure. Lower-right inset: Histogram of the diameter of InN nanowires grown with 20-nm Au clusters. (b) High-resolution TEM image of single-crystalline InN nanowires showing the lattice fringes. The distance of 0.579 nm between two adjacent fringes corresponds to space of (001) planes, which reveals the growth direction (white arrow) perpendicular to [001] direction.

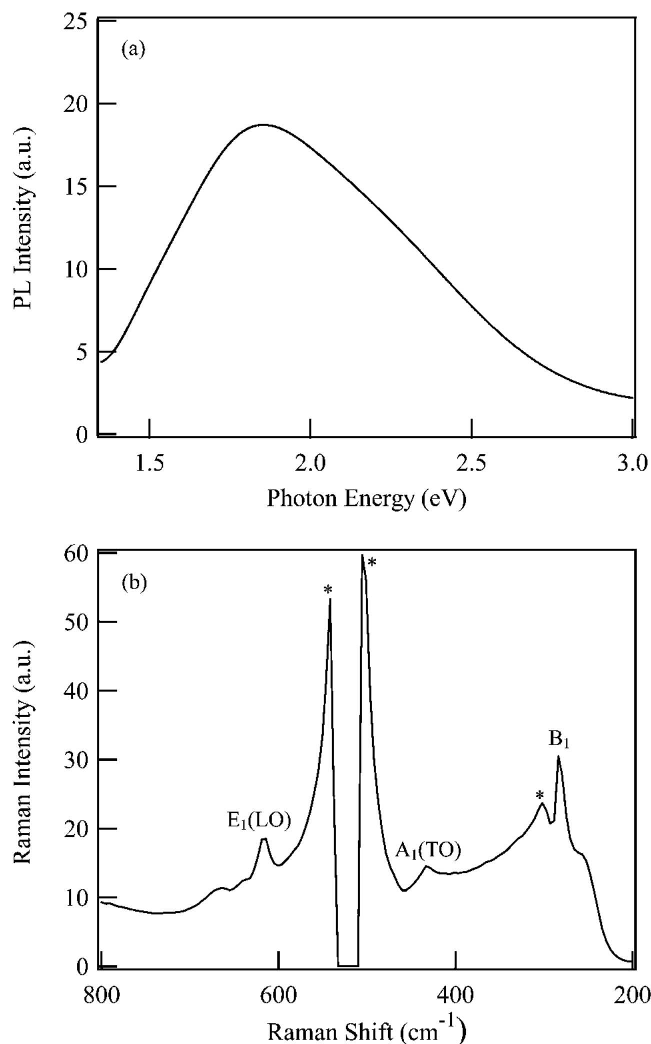

FIG. 3. (a) InN nanowire photoluminescence at the 442 nm excitation. (b) InN nanowire Raman spectrum excited at 442 nm (* denotes peaks from the Si substrate).

20.8 nm and a standard deviation of 7.3 nm. The concentrated distribution centering on the catalytic particle size (20 nm) convincingly proves the VLS growth mechanism and demonstrates the diameter-control capability of our synthesis method. Careful examination of the histogram reveals that 73% of our nanowires have diameters in the range of 15–30 nm. This compares well with the distribution of 10–100 nm in Ref. 5 and 40–80 nm in Ref. 6.

Photoluminescence (PL) and Raman spectra were carried out to characterize the photonic properties of our nanowires using a ultraviolet System 1000 Spectrometer (Renishaw Product Inc., Gloucestershire, UK) in backscattering configurations at room temperature. Figure 3(a) shows a typical PL spectrum measured from a large quantity of InN nanowires on a Si/SiO_2 substrate. The PL emission displays a strong broad peak around 1.85 eV, in agreement with previously reported values.[6] We did not observe the N deficiency or interstitial emission in the 325–780 nm range. It is known that bulk InN (direct band gap $E_g = 1.9$ eV) does not exhibit photoluminescence at room temperature due to the defects induced by the low dissociation temperature, whereas high-quality thin InN films grown via molecular-beam epitaxy showed band-edge PL of 1.81 eV to 2.08 eV below 200 K.[10] Our room-temperature photoluminescence results thus indicate the high quality of our InN nanowires. In addition, our room-temperature Raman analysis shown in Fig. 3(b) at 442 nm excitation showed characteristic B_1 at 283 cm^{-1} (FWHM = 9 cm^{-1}) and A_1 (TO) mode at 431 cm^{-1} (FWHM = 9 cm^{-1}). A_1 (LO) mode at 586 cm^{-1} is buried in the tail of the Si peak at 520 cm^{-1}. In particular, we report the longitudinal optical mode E_1 (LO) at 616 cm^{-1} (FWHM = 12 cm^{-1}). This Raman mode has been predicted by theoretical studies of the hexagonal InN

structures[11]; however, previously it was only observed in the low-temperature Raman analysis.[12] The broad peak at 662 is likely due to the second-order Raman modes. Full width at half-maximum (FWHM) of all other observed Raman modes are very narrow, suggesting very good crystallinity for the InN nanowires, which is consistent with the SAED results.

The synthesis and material analysis were followed by investigations of the electronic properties of our InN nanowires. The as-grown InN nanowires were sonicated into a suspension in isopropanol and then deposited onto a degenerately doped silicon wafer covered with 500 nm SiO_2. Photolithography was performed, followed by evaporating Ti/Au to contact both ends of the nanowires. The upper-left inset of Fig. 4 shows a typical SEM image of our device, indicating a channel length of 2 μm between the source and drain electrodes. Devices consisting of individual nanowire were chosen for detailed analysis.

Figure 4 shows a family of current–voltage (*I–V*) curves of the device measured under various temperatures. A progressive reduction of the device conductance was observed as the temperature decreased. The device exhibited linear *I–V* characteristics at 250 K with a zero-bias resistance of 1.05 MΩ, corresponding to a conductance of 951.5 nano Siemens (nS). When the sample was gradually cooled down, the derivative conductance at zero bias was monotonically reduced to 66.6 nS at 10 K, as shown in the figure. The Fig. 4 inset shows a plot of the zero-bias conductance in logarithm scale as a function of 1000/*T*. The data points for temperatures between 290 K and 50 K can be well-fitted into the formula $G \sim \exp(-E_a/k_B T)$ with E_a approximately 7.5 meV (the solid line), therefore suggesting thermal activation of carriers as the dominant transport mechanism. However, the conductance below 50 K appeared to deviate from the exponential fit. It is suggested that quantum mechanical tunneling turned to dominate over the thermal emission at low temperatures. Similar behavior was previously observed with CdO nanoneedle devices.[13]

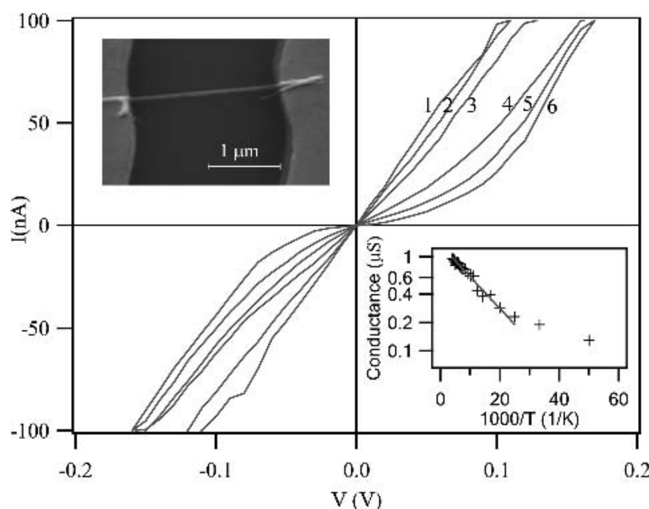

FIG. 4. Curves 1, 2, 3, 4, 5, and 6 correspond to *I–V* measurements of an InN nanowire device obtained at temperatures of 250, 150, 100, 70, 40, and 10 K, respectively. Upper-left inset: SEM image of the measured nanowire device. Lower-right inset: a semi-log plot of conductance versus 1000/*T*. The solid line is a fit using $G \sim \exp(-E_a/k_B T)$ with an activation energy of $E_a = 7.5$ meV.

In summary, we have successfully synthesized single-crystalline InN nanowires using a two-zone chemical vapor deposition technique. A growth rate as high as 4–10 μm/h was achieved due to ample nitrogen radicals supplied by our two-zone system. Precise control over the nanowire diameters was achieved by utilizing gold clusters with well-defined diameters as the catalyst. The crystallinity of the InN nanowires was further confirmed via room-temperature photoluminescence and Raman analysis. In addition, devices based on single nanowires were fabricated, and their electronic transport properties were carefully investigated. Thermal-activated transport was verified to be the dominating transport mechanism for our InN nanowire devices with an activation barrier of 7.5 meV. Our results clearly show the potential of using InN as building blocks for future nanoscale electronics and optoelectronics.

ACKNOWLEDGMENTS

Prof. Edward Goo and the USC Microscope Center are acknowledged for the use of their facilities. This work was supported by USC, NASA Contract No. NAS2-99092, NSF CAREER award, NSF CENS program, and a Zumberger award.

REFERENCES

1. D.A. Neumayer and J.G. Ekerdt, Chem. Mater. **8,** 9-25 (1996).
2. S. Strite and H. Morkoc, J. Vac. Sci. Technol. B **10,** 1237 (1992).
3. S.K. O'Leary, E. Foutz, M.S. Shur, U.V. Bhapkar, and L.F. Eastman, J. Appl. Phys. **83,** 826–829 (1998).
4. Y. Huang, X. Duan, Y. Cui, and C.M. Lieber, Nano Lett. **2,** 101 (2002).
5. J. Zhang, L. Zhang, X. Peng, and X. Wang, J. Mater. Chem. **12,** 802 (2002).
6. C. Liang, L. Chen, J. Hwang, K. Chen, Y. Hung, and Y. Chen, Appl. Phys. Lett. **81,** 22 (2002).
7. S. Han, W. Jin, T. Tang, C. Li, D. Zhang, X. Liu, J. Han, and C. Zhou, J. Mater. Res. **18,** 245 (2003).
8. M.S. Gudiksen and C.M. Lieber, J. Am. Chem. Soc. **122,** 8801 (2000).
9. A. Zubrilov, in *Properties of Advanced Semiconductor Materials GaN, AlN, InN, BN, SiC, SiGe*, edited by M.E. Levinshtein, S.L. Rumyantsev, and M.S. Shur (John Wiley & Sons Inc., 2001) pp. 49–66.
10. T. Yodo, H. Yona, H. Ano, D. Nosei and Y. Harada, Appl. Phys. Lett., **80,** 968 (2002).
11. G. Kaczmarczyk, A. Kaschner, S. Reich, A. Hoffmann, C. Thomsen, D.J. As, A.P. Lima, D. Schikora, K. Lischka, R. Averbeck, and H. Riechert, App. Phys. Lett., **76,** 2122 (2000).
12. Z.G. Qian, G. Yu, W.Z. Shen, H. Ogawa, Q.X. Guo, Physica B, **318,** 180 (2002).
13. X. Liu, C. Li, S. Han, J. Han, C. Zhou, Appl. Phys. Lett. **82,** 1950 (2003).